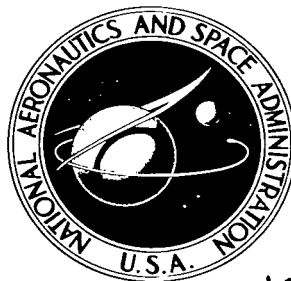


NASA TECHNICAL NOTE

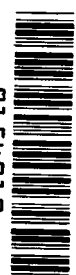


NASA TN D-2396

c. 1

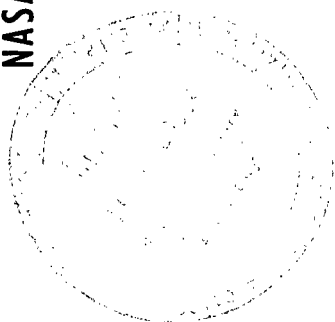
LOAN COPY: RETL
AFWL (WLIL-
KIRTLAND AFB, N

0154910



TECH LIBRARY KAFB, NM

NASA TN D-2396



EXPERIMENTAL DETERMINATION OF THE
DEPENDENCE OF CRACK EXTENSION FORCE
ON CRACK LENGTH FOR A SINGLE-EDGE-NOTCH
TENSION SPECIMEN

*by John E. Srawley, Melvin H. Jones,
and Bernard Gross*

*Lewis Research Center
Cleveland, Ohio*



EXPERIMENTAL DETERMINATION OF THE DEPENDENCE OF
CRACK EXTENSION FORCE ON CRACK LENGTH FOR A
SINGLE-EDGE-NOTCH TENSION SPECIMEN

By John E. Srawley, Melvin H. Jones, and Bernard Gross

Lewis Research Center
Cleveland, Ohio

NATIONAL AERONAUTICS AND SPACE ADMINISTRATION

For sale by the Office of Technical Services, Department of Commerce,
Washington, D.C. 20230 -- Price \$0.50

EXPERIMENTAL DETERMINATION OF THE DEPENDENCE OF
CRACK EXTENSION FORCE ON CRACK LENGTH FOR A
SINGLE-EDGE-NOTCH TENSION SPECIMEN

by John E. Srawley, Melvin H. Jones, and Bernard Gross

Lewis Research Center

SUMMARY

The single-edge-notch form of a plane-strain (or opening mode) crack toughness specimen is particularly economical in regard to available test material and testing machine capacity. The necessary calibration relation for a particular design of a single-edge-notch specimen, centrally loaded in tension, was determined from a series of compliance measurements at crack lengths ranging from zero to one-half the specimen width. The accuracy of the calibration is estimated to be $\pm 1/2$ percent in the range of interest. Agreement with concurrent results obtained by boundary collocation of an appropriate stress function is excellent. Alternative types of specimen are discussed, and the relation between necessary specimen size and the ratio of toughness to yield strength is emphasized.

INTRODUCTION

In order to determine the fracture toughness (\mathcal{G}_c or K_{Ic}) of materials by means of tests on specimens provided with simulated cracks, it is first necessary to establish an expression that relates the strain-energy release rate (crack extension force) \mathcal{G} or the stress intensity factor K to the specimen dimensions and the applied load (ref. 1). The alternative methods for obtaining a sufficiently accurate expression for a given specimen design are (1) mathematical stress analysis procedures (refs. 2 and 3); (2) experimental stress analysis procedures, utilizing photoelasticity or resistance strain-gage techniques; and (3) experimental measurements of specimen compliance as a function of crack length (refs. 3 and 4). This report is concerned with the application of the third of these methods to a flat-plate specimen containing a single-edge notch and subjected to tensile loading.

The single-edge-notch specimen is specifically intended for measurement of the plane-strain crack toughness K_{Ic} and is not considered suitable for measurement of mixed mode or plane-stress K_c values (refs. 1, 2, 3, and 5). In simple terms, K_{Ic} can be regarded as the lower limiting value to which the

K_{IC} of a plate material tends as the thickness is increased so that fracture occurs almost entirely in the transverse or opening mode with negligible oblique shear borders. The K_{IC} toughness is of particular importance as a simple index of the toughness of a material, which is the controlling value in many engineering failures.

Measurement of the K_{IC} of many materials of engineering importance requires careful selection of specimen design in order to keep the specimen dimensions as small as possible, consistent with accuracy, and in order to avoid having to use very large testing machines. The single-edge-notch specimen was selected because it has particular advantages in these respects. The following section provides more detailed background information on the measurement of plane-strain crack toughness and on the comparison of the single-edge-notch specimen with other specimen designs that could be used for this purpose.

SYMBOLS

a	crack length in single-edge-notch specimen
C	compliance per unit thickness of a specimen, or of a section of the length of a specimen; equal to change in length of selected section per unit change in P
D	diameter
E	Young's modulus
e	displacement corresponding to P of the point of application of P strain energy release rate with crack extension, or, crack extension force (refs. 1, 2, and 3)
K	stress intensity factor of elastic stress field in vicinity of border of a crack (refs. 1, 2, and 3)
k	degree of polynomial
n	number of data points
P	load per unit thickness applied to specimen
W	width of single-edge-notch specimen
ν	Poisson's ratio
σ_{ys}	0.2-percent-offset tensile yield strength

Subscripts:

c	critical value at onset of rapid fracture, taken to be measure of fracture toughness
I	first or opening mode of crack extension

BACKGROUND

The plane-strain crack toughness of a material is a measure of its resistance to crack extension under conditions of maximum constraint, as in the ideal case of a crack completely embedded in a large bulk of the material under tension normal to the crack plane. Irwin has distinguished three component modes of crack extension that can be linearly combined to represent any arbitrary mode (refs. 2 and 3). These modes are designated by the subscripts I, II, and III; the first or opening mode corresponds with the alternative measures of plane-strain crack toughness K_{Ic} and \mathcal{G}_{Ic} . For plane strain,

$$\mathcal{G} = \frac{K^2(1 - \nu^2)}{E}$$

where E is Young's modulus and ν is Poisson's ratio. For plane stress,

$$\mathcal{G} = \frac{K^2}{E}$$

As pointed out in references 2 and 3, the question of what combination of the component modes of crack extension will occur in any particular case is a matter to be decided by observation rather than by mathematical analysis. The opening mode appears to be of primary interest in that it dominates in many cases of engineering importance, most obviously in cases of so-called brittle fracture. Even in cases of thin structural members that exhibit fractures with substantial oblique shear borders, the initial, critical stage of crack extension may have occurred in the opening mode and thus may have been controlled by K_{Ic} (ref. 5). Furthermore, the plane-strain crack toughness is more uniquely characteristic of a material than is any measure of mixed-mode crack toughness because it is not dependent on section thickness as such, that is, except insofar as the section thickness influences the effects of metallurgical processing variables. For these reasons, the development of methods of measurement of plane-strain crack toughness that are both practicable and sufficiently accurate is a matter of some current importance.

Any crack toughness test is simply a model fracture experiment on a suitable specimen that has been provided in advance with a simulated crack. The specimen is so designed that the value of the stress intensity factor at the onset of rapid crack extension can be calculated from the observed load and the dimensions of the specimen and the crack on the basis of a preestablished stress analysis, which may be either theoretical or obtained by the experimental procedure described later. To obtain a plane-strain toughness value the observations must correspond with onset of rapid fracture in the opening mode. The calculation basis is only valid when the specimen behavior is substantially elastic, except for a restricted yielded zone in the vicinity of the crack. This requirement imposes a strict limitation on how small a specimen may be used to obtain a valid crack toughness measurement. In fact, for any given specimen design, the dimensions required increase in proportion to the square of the ratio of the K_{Ic} to the yield strength of the material. This squared ratio is a measure of the critical crack size for fracture at some fixed fraction of the yield strength depending on the design of the specimen.

This specimen size limitation is a serious handicap in the attempt to extend the measurement of crack toughness over the entire range of engineering materials of practical interest. For instance, in the case of the familiar round notched bar of diameter D and notched diameter $0.707D$, if it is assumed that a useful K_{Ic} measurement will result as long as the net fracture stress is less than 1.2 times the yield strength, a conservative calculation (neglecting plastic-zone correction) suggests that D has to be greater than about $4(K_{Ic}/\sigma_{ys})^2$. Results obtained by Boyle, Sullivan, and Krafft with aluminum 7075.T6 round notched bars of various diameters are consistent with this rough estimate (ref. 6). On the basis of this estimate, and projecting from available data on higher strength steels, it can be anticipated that there will be steels having yield strengths exceeding 150,000 psi, which would require notched round bar diameters in excess of 4 inches for valid K_{Ic} measurements. Tests of such large specimens are feasible only when the following conditions can be satisfied: (1) the material is available in sufficiently heavy stock; (2) the metallurgical characteristics of the heavy stock do not differ substantially from those of the stock to be used in the anticipated application (such factors as grain size, heterogeneity, isotropy, and response to heat treatment must be considered); (3) any special facilities needed for treating specimens must be of sufficient capacity, for instance, space in a test reactor for studying irradiation effects; and (4) the capacity of available machines for testing and fatigue cracking the specimens must be sufficient.

Because these limitations of the notched round specimen were recognized, the suitability of symmetrically edge- or center-notched flat specimens for K_{Ic} measurement was investigated in reference 6. This suitability depends on unambiguous determination of the load at which rapid crack extension in the opening mode first occurs. The corresponding value of \mathcal{G} can be regarded as numerically equal to the controlling value of \mathcal{G}_I , and the corresponding K_{Ic} can be taken to represent the K_{Ic} of the material. Subsequent to this so-called "pop-in" load, the specimen may sustain considerable further loading before fracturing completely because of the relief of elastic constraint by plastic contraction of the thickness of the specimen in the vicinity of the crack front. This relief of constraint has the effect of suppressing further crack propagation in the opening mode and favoring development of oblique, mixed-mode fracturing. If the specimen is thick enough, however, the initial opening mode crack extension will be sufficiently extensive to permit detection of the load at which it occurs by one or other of several techniques. It was found in reference 6 that tests of flat specimens of the aluminum 7075.T6 alloy, which were both sufficiently wide and thick, gave K_{Ic} values in good agreement with these obtained from round notched bars of sufficiently large diameter. The minimum required width of a flat specimen was about the same as the minimum required diameter of a notched round bar. The minimum thickness for distinct "pop-in" detection was about one-fifth of the minimum required width. While these findings apply to tests on one particular material and should not be assumed to have unlimited validity for all materials, they do indicate that the symmetrically notched flat specimen has a marked advantage over the notched round specimen in respect to cross-sectional area and load requirement for testing. The flat specimen has a particular advantage when the material stock to be tested is in the form of a plate. In this case, as can be deduced from the preceding discussion, the maximum level of K_{Ic}/σ_{ys} , which could be mea-

sured with a flat specimen of thickness equal to that of the plate would be more than twice that of a round bar machined from the plate.

The symmetrically notched flat specimen can be visualized as a central, longitudinal slice of a round notched bar. It is then apparent that the approximate equivalence between width and diameter is to be expected.

The single-edge-notch specimen was proposed by Irwin, Krafft, and Sullivan as a further economy in specimen material and load requirement (memorandum to the ASTM Special Committee on Fracture Testing of High Strength Metallic Materials, August 21, 1962). This specimen can be visualized as derived from the symmetrical flat specimen by cutting it in half along the longitudinal centerline and shortening it accordingly. Since this operation does not affect either the thickness or the simulated crack size, it would appear that the K_{IC}/σ_{ys} measurement capacity should be about the same for the single-edge-notch specimen as for the symmetrical specimen of the same thickness. The width and length of the single-edge-notch specimen are half those of the symmetrical specimen, while the load requirement is considerably less than half, depending on the asymmetry of loading with respect to the centroid of the net section in the plane of the notch.

In view of the anticipated relatively high efficiency of the single-edge-notch specimen for K_{IC} measurement and the consequent likelihood that it will be widely used, the basis for calculating K_{IC} values from the test data must be established with adequate accuracy. Because a theoretical stress analysis of the specimen from which the required relation could be derived was lacking, the alternative was to employ an experimental compliance measurement procedure, which was originally suggested by Irwin and Kies (ref. 4). Although the re-

sults of a compliance calibration for a single-edge-notch specimen have previously been published by Sullivan (ref. 7), there is some question regarding the accuracy of this calibration because of the small size of the specimens and certain features of the procedure. Therefore obtaining a more refined calibration by utilizing every reasonable means of attaining maximum accuracy was desirable.

Since the completion of the experimental work, Gross, Srawley, and Brown have been successful in applying boundary collocation procedures to a suitable stress function to obtain a mathematical solution to the problem (ref. 8). The results obtained in this way are in satisfactory agreement with the experimental results, as will be shown in the section Comparison with Stress Function Solution Values.

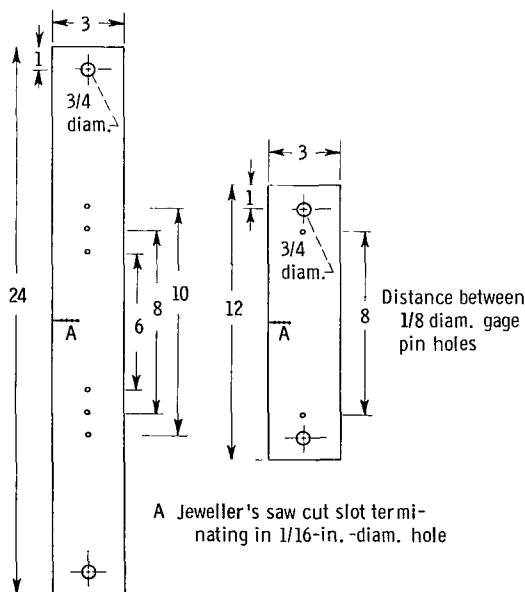


Figure 1. - Calibration specimens of 1/2-inch-thick aluminum 7075-T6 plate.

CALIBRATION PRINCIPLE

If an axially loaded plate specimen of width W , such as is shown in figure 1, with a central, transverse slit of length a extending from one edge to represent a crack is considered, it can be shown (ref. 4) that the strain energy release rate with crack extension is given by

$$\mathcal{G} = \frac{P^2}{2} \frac{dC}{da} \quad (1)$$

where P is the applied force per unit thickness and C is the total compliance of the specimen per unit thickness e/P ; e is the displacement corresponding to P of the point of application of P .

It is convenient to express this relation in the dimensionless form

$$\frac{EW\mathcal{G}}{P^2} = \frac{E}{2} \frac{dC}{d(a/W)} \quad (2)$$

where E is Young's modulus.

The experimental calibration procedure consists of making a series of measurements of C for a sufficient number of values of a/W to permit accurate determination of $dC/d(a/W)$ over the range of interest. The measurements must be made in the essentially elastic range, so that the displacements are recoverable on unloading. Equation (2) is independent of specimen thickness, because \mathcal{G} is defined in terms of unit length of crack border and P and C are defined in terms of unit plate thickness, and it is also independent of the size scale of the other specimen dimensions. Thus, the calibration relation will apply to a specimen of any size providing it has the same proportions as the specimen used in obtaining the calibration except for thickness, which may have any value. The relation is also independent of the elastic properties of the specimen material.

Once the calibration has been conducted with a satisfactory degree of accuracy, all that needs measuring in a crack toughness test are the values of P and a/W corresponding to onset of rapid crack extension in the opening mode. Reference is then made to the plot or table of values of $EW\mathcal{G}/P^2$ against a/W , and the appropriate value is used to calculate \mathcal{G} . A suitable plastic zone correction (see ref. 1) can be incorporated either by iteration or by a graphical solution procedure.

The exact manner in which a value of K_{Ic} should be calculated to correspond with a value of \mathcal{G} obtained in this way is open to some question. This point was discussed by the authors with G. R. Irwin, and, although of minor importance for practical purposes, should be kept in mind. The state of stress in a cracked plate specimen is one of generalized plane stress except within a very restricted region where the constraining influence of the crack induces a state approaching plane strain. The ratio of this constrained volume to the total volume from which strain energy is released as the crack extends

is quite small. Consequently, in comparing \mathcal{G} values derived from experimental compliance measurements with K values derived from a two-dimensional stress analysis procedure, as is done in the section Comparison with Stress Function Solution Values, the plane-stress relation $K^2 = E\mathcal{G}$ is appropriate.

In regard to an actual crack toughness test, however, it can be argued from physical considerations that the stress intensity prevailing in the region where opening mode crack instability occurs is not properly represented by a two-dimensional stress analysis and, in fact, will exceed the value obtained by such a procedure. It seems likely that the difference would amount to no more than the difference between the plane-stress and the plane-strain relation $K^2 = E\mathcal{G}/(1 - \nu^2)$. This difference amounts to approximately 5 percent in the value of K . Unfortunately, because there is no experimental or analytical basis at present for assuming either this extreme or some intermediate value, some arbitrary decision has to be made. For consistency with the previous practice, the best course seems to be to follow the precedent established in reference 6 of assuming the plane-strain relation for purposes of calculating K_{Ic} values from "pop-in" \mathcal{G} measurements.

CALIBRATION PROCEDURE

General Considerations

The earlier calibration procedure presented in reference 7 consisted of obtaining autographic records of the change in distance between loading pin centers against load. A standard microformer extensometer was used for this purpose. The procedure began with an unslotted specimen and was repeated for progressively deeper slots so that a sufficient number of slope measurements could be made. The resulting values of C were plotted against the slot length a , and values of dC/da were estimated by visual fitting of tangents to a smooth curve fitted to the data points.

The present investigators considered that the procedure of reference 7 involved possibilities of appreciable errors that could be reduced considerably by refinements of technique. The most likely source of error appeared to be the large and somewhat uncertain contribution to the total specimen compliance from the loading pin-hole regions where high stress concentrations occur. In fact, the compliance value measured for the unslotted specimen indicates that the major contribution to the measured compliance was from the distortion of the loading pin holes. (The compliance value to be expected for this case, assuming no hole distortion or bending of the pins, can easily be calculated from the known value of Young's modulus.)

This difficulty can be circumvented by measuring the compliance of a sufficiently long central section of the specimen rather than making the measurement between loading pin centers. If the length of the central section is sufficient, the compliance of the remainder of the specimen will be virtually independent of a/W , and $dC/d(a/W)$ for the central section will be the same as for the entire specimen. The sufficient length for the central section must, of course, be accurately established. A preliminary, rough estimate of

the minimum necessary gage length was obtained by photoelastic model experiments. The fringe patterns indicated that the gage length should not be less than four times the length of the longest slot to be used. To determine more precisely whether the effect of gage length would be appreciable beyond this estimated necessary minimum, preliminary compliance measurements were made on a specimen 24 inches long by 3 inches wide over gage lengths of 6, 8, and 10 inches for slots up to 1.5 inches long (fig. 1). As will be shown later, these measurements established that there was no systematic difference between values of dC/da computed from measurements made over these three gage lengths. Hence, for an accurate calibration covering a range of values of a/W up to 0.5, the gage length should not be less than $2W$.

In the interest of the economy of material, the length-to-width ratio of the practical test specimen should be no greater than necessary for an accurate calibration. With allowance made for the shrouding of the ends of the specimen by the loading clevises and with the requirement that the gage length should be not less than $2W$, the optimum ratio of length to width appeared to be about 4. This ratio, which is the same as that recommended by the ASTM Special Committee on Fracture Testing of High Strength Metallic Materials for symmetrically notched specimens (ref. 1), was adopted for the duplicate calibration specimens.

The most critical factor in the calibration procedure is the accuracy of the displacement measurements, and since the magnitudes of the maximum permissible displacements are proportional to the specimen size scale, it would appear that the larger the specimen the more accurate the calibration. Sullivan used specimens that were only about 1 inch wide by 2 inches long, which is a second factor restricting the accuracy of her calibration. In the present work, the dimensions of the duplicate calibration specimens, 3 inches wide by 12 inches long with a gage length of 8 inches (fig. 1), were chosen so that the displacement measurements could be made with an expected accuracy of not less than $\pm 1/2$ percent. The 0.5-inch thickness could be measured with an accuracy of 0.1 percent.

The choice of material also affects the accuracy of the displacement measurements. The best material would be that with the largest range of purely elastic strain, indicated roughly by the ratio of yield strength to Young's modulus. Of the readily available, easily machined materials, aluminum 7075-T6 appeared to be the most satisfactory. This material has a yield-to-modulus ratio of about 0.007. Certain nonmetallic materials of low modulus might have been better, but they were not used because of the lack of sufficient information on elastic range, stability, brittleness, and homogeneity.

Measurement Details

In each case the compliance of the unslotted specimen was measured first. The specimen was then removed from the testing machine, and a $1/16$ -inch-diameter hole was so drilled that its center was on the lateral centerline of the specimen and 0.50 inch from one edge. This hole was then joined to the edge by cutting with a jeweller's saw along the lateral centerline. The diameter of the hole and the distance from the edge of the specimen to the extrem-

ity of the hole were then measured on an optical comparator. This slot was considered to represent a line discontinuity, or ideal crack, equal in length to the total length of the slot minus one-half the radius of the terminating hole. This concept, due to G. R. Irwin, assumes that the slot is equivalent to an extremely prolate semiellipse having a terminal radius of curvature equal to that of the hole. It is further assumed that the effect of such a semielliptical notch on the specimen compliance would be virtually the same as that of any other member of the family of confocal semiellipses with a smaller terminal radius of curvature, the limiting case being the line joining the center to the focus. It can be shown that the distance from the focus to the end of the major axis of an ellipse approaches a value equal to one-half of the terminal radius of curvature as the ratio of minor to major axis approaches zero. The manner of calculating the effective crack length then follows. The use of a well-defined radius rather than a sharp notch to terminate the slot allows more precise definition of the equivalent crack length, which would otherwise be located somewhere within an ill-defined plastically deformed region surrounding the notch tip. The hole diameter should, of course, be as small as possible consistent with elastic behavior of the surrounding material. For the specimen dimensions used in this case, a 1/16-inch-diameter hole has negligible effect on the total elastic strain energy of the specimen.

After measuring the compliance of the specimen for this slot length, the procedure was repeated a number of times. A new hole was drilled each time and the cut extended to join the hole to the specimen edge. The positions of the holes were such as to correspond to values of a/W of approximately 0.172, 0.252, 0.279, 0.305, 0.332, 0.359, 0.385, 0.412, 0.455, and 0.500, covering the range up to 0.500, but with concentration on the central range, 0.25 to 0.41, which is of the most practical interest.

To measure the compliances, the specimens were loaded in a tensile testing machine of 200,000-pounds maximum capacity. The load was transmitted to the specimens through pins that minimized bending in one plane; the loading train also incorporated pin joints to minimize bending in the conjugate plane. In each case the maximum load applied was a major fraction of the testing machine range selected so that the precision of load measurement was as great as possible. The load measurement accuracy was at least $\pm 1/4$ percent.

The displacements were measured with the specially constructed beam gages shown in figure 2. These gages consist essentially of strips of titanium - 13-V-11Cr-3Al alloy, approximately 5 inches long by 0.5 inch wide by 0.060 inch thick, with epoxy-backed foil resistance gages of 1-inch gage length bonded to each side. In use, the beam gages are bent and span the distance between the stepped blocks that are located on the specimen by means of 1/8-inch-diameter pins passing through the blocks and the specimen, as

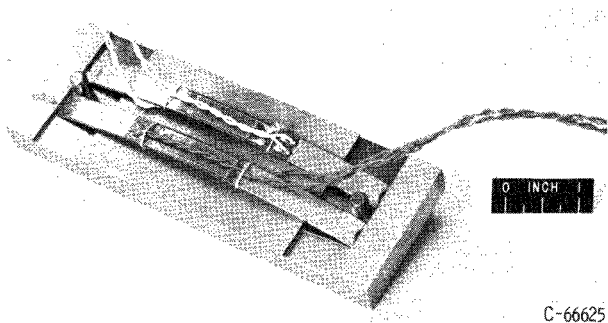
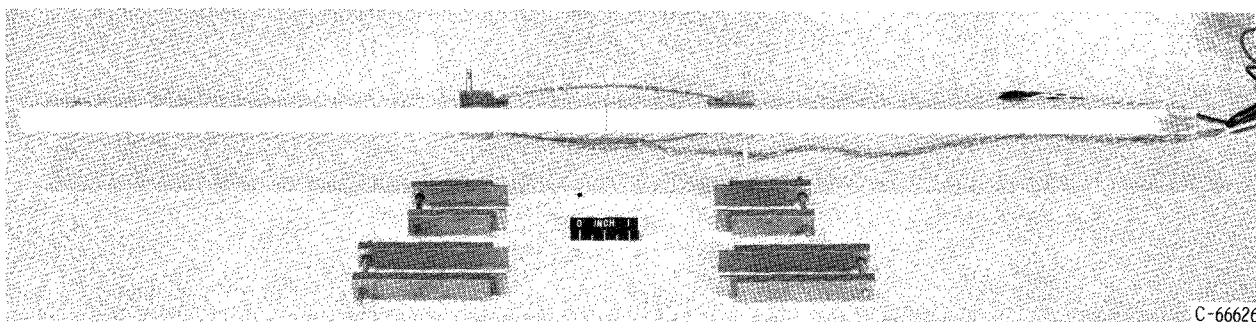


Figure 2. - Beam gages used for displacement measurements mounted in keeper block.



C-66626

Figure 3. - Beam gages mounted on specimen utilizing shortest filler blocks to make up a gage length of 6 inches. Filler blocks for other gage lengths in foreground.

shown in figure 3. Blocks of different sizes were used to make up 6-, 8-, or 10-inch total gage lengths as required; the same pair of beam gages were used for all measurements. A commercial strain-gage indicator was used to measure the beam-gage strain, as indicated by the resistance gages. The beam gages were calibrated with a supermicrometer and had a sensitivity exceeding 100 indicated microstrain units per 0.001-inch change in span. The displacement measurement precision was estimated to be ± 0.00003 inch. In order to eliminate zero drift of the gages arising from creep of the resistance gage bonding material, large changes in deflection must be avoided. Therefore the gages were kept deflected in a keeper block when not in use (fig. 2) and were manipulated with a special handling device when they were placed in position on the specimens. A zero reading was always made on each gage before removal from the keeper block. This reading did not change more than 10 microstrain units throughout the series of compliance measurements.

Compliance Measurement Procedure

After a specimen was set up in the testing machine prior to each actual compliance measurement run, the specimen was loaded to the maximum that would be applied for the compliance measurement (30, 25, 20, 15, 12, or 10 thousand lb, depending on the value of a/W), unloaded, reloaded, and again unloaded. The purpose of this procedure was to ensure that any slight degree of inelastic behavior had been eliminated by work hardening of the material in the immediate vicinity of the end of the slot. Load-extension curves from a microformer extensometer straddling the slot were autographically recorded; the slight hysteresis occurring in the first loading cycle did not occur in the second cycle.

After this shake-down procedure, the load was again applied slowly, and the output from one of the beam gages was measured and recorded at regular load intervals up to maximum load. Certain measurements were repeated on unloading. This cycle was then repeated, but the output from the other beam gage was measured. The two sets of results were then compared to determine the degree of agreement. A difference of less than 2 percent in the slopes of the load-displacement plots was considered satisfactory, and the average slope was then taken as the compliance. Any greater difference was considered to indicate excessive bending of the specimen. In the few cases in which this was ob-

served, the runs were repeated with satisfactory results after adjusting the loading train. Typical examples of load-displacement plots are shown in figure 4.

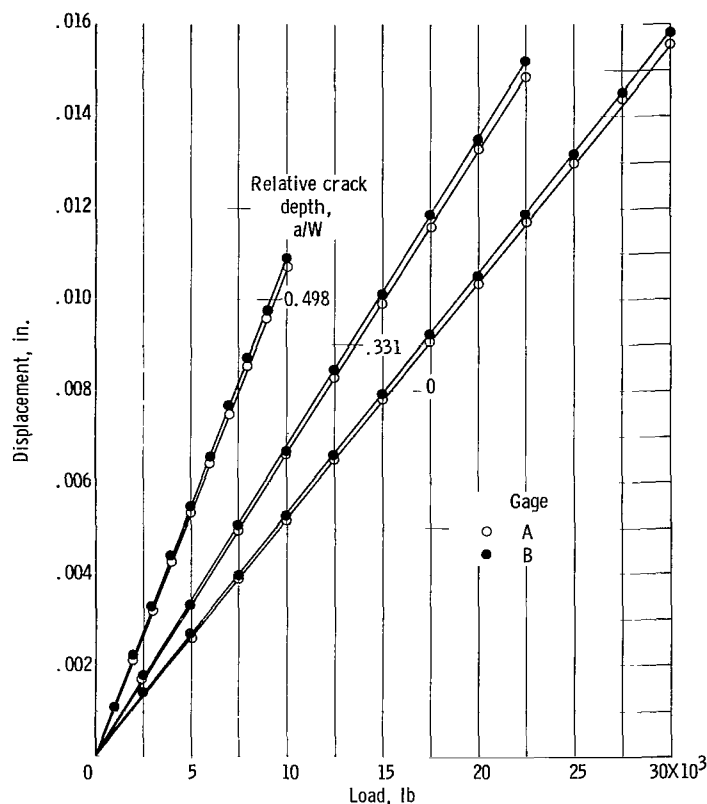


Figure 4. - Typical load-displacement plots for 12-inch-long specimens with 8-inch gage length.

Two supplementary measurements were made during each run. An autographic load-extension record was obtained from a 2-inch-gage-length microformer extensometer straddling the slot and close to the edge of the specimen. These records provided data useful in making actual K_{Ic} tests in which an equivalent gage would be used to sense extension of the crack. The second measurement was concerned with the extent of bending in the plane of the specimen, which causes the end of the slot to be displaced from its initial position with respect to the axis of loading in proportion to the magnitude of the load. For a given slot length, this displacement per unit load is proportional to the distance between loading centers, that is, proportionately greater for a long specimen than for a short one. The result is that the ratio of specimen length to width has a small but appreciable effect on $dC/d(a/W)$. The

measurement of the extent of bending was made by holding a straight edge against the unslotted edge of the loaded specimen and measuring the gap with feeler gages. The results will be referred to in the section Comparison with Stress Function Solution Values.

Treatment of Data

The results of the compliance measurements on the 24-inch-long specimen and on the duplicate 12-inch-long specimens are given in table I in the form of values of $EC/2$ against a/W , where C is the compliance per unit thickness and E is Young's modulus (taken to be 10,300,000 psi). The compliance measurements are estimated to be accurate within about $\pm 1/2$ percent, based on the estimated accuracies of the load, displacement, and dimensional measurements involved. This estimated accuracy may be compared with the root-mean-square percentage difference of the $EC/2$ values for the duplicate 12-inch specimens, which is 0.39 percent (using linear interpolation to adjust the

TABLE I. - MEASURED VALUES OF $EC/2$ AGAINST a/W FOR 24-INCH-
LONG SPECIMEN AND DUPLICATE 12-INCH-LONG SPECIMENS

Specimen length, in.									
24				12					
a/W	Gage length, in.			(a)		(b)			
	6	8	10	a/W	Gage length, in.	a/W	Gage length, in.		
					8		8		
								EC/2	EC/2
0	1.017	1.357	1.691	0	1.348	0	1.352		
.173	1.098	1.433	1.762	.170	1.424	.171	1.433		
.252	1.199	1.534	1.881	.251	1.532	.252	1.539		
.279	1.249	1.593	1.927	.278	1.581	.278	1.585		
.305	1.308	1.649	1.984	.305	1.659	.305	1.658		
.333	1.382	1.722	2.065	.331	1.729	.329	1.730		
.359	1.478	1.824	2.159	.359	1.838	.358	1.836		
.385	1.582	1.921	2.258	.386	1.944	.387	1.963		
.413	1.733	2.078	2.404	.412	2.088	.411	2.085		
.456	2.033	2.369	2.707	.456	2.387	.456	2.399		
.497	2.381	2.731	3.063	.498	2.775	.498	2.788		

values of $EC/2$ to correspond with a common set of values of a/W).

A number of measurements of Young's modulus were made on specimens from the same piece of plate as the compliance calibration specimens. The most consistent set of values was obtained by using the 5-inch beam gages over a gage length of 5.390 inches on a specimen of 0.5-inch square cross section. The gages were held between yokes attached to the specimen with pointed set screws. The average of 10 measurements was 10,300,000 psi with a standard deviation of 40,000 psi. This value

agrees well with the handbook value for 7075-T6, which is given as 10,400,000 psi for the average of tension and compression measurements; the tension modulus is about 2 percent less than that for compression.

Each of the sets of data in table I was fitted in turn to polynomials in a/W of degrees 3, 4, 5, 6, and 7 by means of a least-squares-best-fit digital computer program. The program was

TABLE II. - COMPARISON OF EXPERIMENTAL DATA WITH
COMPUTED VALUES OF $EC/2$ ACCORDING TO DEGREE
OF FITTING POLYNOMIAL FOR SPECIMEN 12a

a/W	Data	Degree of fitting polynomial				
		3	4	5	6	7
		$EC/2$				
0	1.348	1.376	1.346	1.348	1.348	1.348
.170	1.424	1.405	1.428	1.422	1.423	1.424
.251	1.532	1.510	1.533	1.533	1.532	1.532
.278	1.581	1.569	1.586	1.588	1.587	1.587
.305	1.659	1.643	1.651	1.654	1.654	1.653
.331	1.729	1.729	1.728	1.730	1.730	1.730
.359	1.838	1.841	1.829	1.831	1.832	1.832
.386	1.944	1.969	1.950	1.949	1.950	1.951
.412	2.088	2.112	2.090	2.088	2.087	2.088
.456	2.387	2.404	2.392	2.388	2.386	2.385
.498	2.775	2.744	2.772	2.775	2.775	2.776

such that the coefficients of the first power of a/W were each forced to be equal to zero on the priori grounds that \mathcal{G} is zero when the crack length is zero. Examination of the results showed that while the fourth-degree polynomials fitted the data substantially better than those of the third degree, there was no further significant improvement with polynomials of higher degree. The criterion of optimum fit was taken to be the sum of the squared residuals divided by the degrees of freedom, $n-k-1$, where n is the number of data points and k is the degree of the polynomial (ref. 9). This index was smallest for the fourth-degree polynomial in each case. A comparison of

TABLE III. - VALUES OF COEFFICIENTS OF THE POLYNOMIALS

$$\frac{E}{2} \frac{dC}{d(a/W)} = \frac{EWg}{pZ} = A_1 \frac{a}{W} + A_2 \left(\frac{a}{W}\right)^2 + A_3 \left(\frac{a}{W}\right)^3$$

Coefficient	Specimen length, in.					
	24			12		12a + 12b
				a	b	
	Gage length, in.					
	6	8	10	8	8	8
A ₁	7.597	7.586	8.342	7.569	7.572	7.586
A ₂	-34.34	-34.02	-38.51	-31.48	-32.10	-31.90
A ₃	120.31	120.07	126.02	115.96	118.19	117.28

are given in table III. In addition, tables of values of $(E/2)[dC/d(a/W)]$ were computed.

DISCUSSION OF RESULTS

Effect of Gage Length

As mentioned earlier in the section Calibration Procedure - General Consideration, the purpose of the 24-inch-long specimen was to establish the minimum necessary gage length such that $dC/d(a/W)$ would be the same over this gage length as for the entire specimen.

TABLE IV. - COMPARISON OF COMPUTED

VALUES OF $\frac{E}{2} \frac{dC}{d(a/W)}$ FOR THREE
DIFFERENT GAGE LENGTHS USED
ON 24-INCH-LONG SPECIMEN

a/W	$\frac{E}{2} \frac{dC}{d(a/W)}$		
	Gage length, in.		
	6	8	10
0	0	0	0
.05	.31	.31	.34
.10	.54	.54	.58
.15	.77	.78	.81
.20	1.11	1.12	1.14
.25	1.63	1.63	1.64
.30	2.44	2.46	2.44
.35	3.63	3.65	3.62
.40	5.24	5.28	5.24
.45	7.43	7.47	7.42
.50	10.25	10.30	10.30

the experimental data with computed values of $EC/2$ for the various polynomials is shown in table II for specimen 12a as an example. This comparison is typical of the comparisons for each of the three specimens.

The fourth-degree polynomials were differentiated with respect to a/W to give $(E/2)[dC/d(a/W)]$ expressed as a third-degree polynomial in a/W for each case. The values of the coefficients of these third-degree polynomials

are given in table III. In addition, tables of values of $(E/2)[dC/d(a/W)]$ were computed. Table IV gives the values of $(E/2)[dC/d(a/W)]$ derived from the data for each of the three gage lengths used with the 24-inch-long specimen. These values correspond to the respective polynomials in table III. While there is an appreciable tendency for $(E/2)[dC/d(a/W)]$ to be slightly higher for the 10-inch gage length than for the 6- or 8-inch gage lengths when a/W is small, there are no systematic differences between the three sets of values when a/W exceeds 0.20. Since the range of a/W of practical interest is from 0.25 to 0.40, this table shows that a gage length of 6 inches or greater is sufficient for a 3-inch-wide specimen.

Practical Test Specimen Calibration Table

It was proposed earlier that the optimum ratio of length to width of the practical test specimen should be about 4. The recommended

calibration is therefore derived from the results from the duplicate 12- by 3-inch specimens. The root-mean-square percentage difference between values of $(E/2)[dC/D(a/W)]$ from the two specimens (computed as described in the previous section) was calculated as 0.70 percent; that is, the root-mean-square deviation

TABLE V. - RECOMMENDED VALUES OF $\frac{E}{2} \frac{dC}{d(a/W)} = \frac{EWg}{P^2}$
FOR PROPOSED SINGLE-EDGE-NOTCH SPECIMEN DESIGN
[Interpolate linearly for intermediate values.]

a/W	$\frac{E}{2} \frac{dC}{d(a/W)}$	a/W	$\frac{E}{2} \frac{dC}{d(a/W)}$	a/W	$\frac{E}{2} \frac{dC}{d(a/W)}$
0	0	0.20	1.180	0.40	5.436
.01	.073	.21	1.273	.41	5.830
.02	.140	.22	1.374	.42	6.248
.03	.202	.23	1.484	.43	6.688
.04	.260	.24	1.604	.44	7.153
.05	.314	.25	1.735	.45	7.641
.06	.366	.26	1.878	.46	8.155
.07	.415	.27	2.031	.47	8.695
.08	.462	.28	2.198	.48	9.261
.09	.510	.29	2.378	.49	9.855
.10	.556	.30	2.571	.50	10.477
.11	.605	.31	2.780		
.12	.653	.32	3.004		
.13	.705	.33	3.245		
.14	.758	.34	3.501		
.15	.816	.35	3.775		
.16	.877	.36	4.069		
.17	.944	.37	4.380		
.18	1.016	.38	4.711		
.19	1.094	.39	5.064		

from the average was 0.35 percent. The recommended values of $(E/2)[dC/d(a/W)] = EWg/P^2$ are given in table V for intervals of a/W of 0.01. These values were derived from the combined results for the two specimens. The last line in table III gives the coefficients of the corresponding polynomial. For all practical purposes, however, intermediate values of the tabulated function may be obtained with sufficient accuracy by linear interpolation between the tabulated values. For this purpose, the values are given to three decimal places, although the accuracy is not expected to be better than $\pm 1/2$ percent. In fact, accuracy of this order is expected only in the range of a/W between about 0.25 and 0.4 because the data points were deliberately concentrated in this range of greatest practical importance.

Comparison with Stress Function

Solution Values

TABLE VI. - COMPARISON OF EXPERIMENTAL AND STRESS FUNCTION SOLUTION VALUES OF $\frac{E}{2} \frac{dC}{d(a/W)}$

a/W	Stress function values, ref. 12	Present work	Sullivan's values, ref. 7
0.05	0.204	0.314	0.35
.10	.445	.556	.65
.15	.758	.816	1.00
.20	1.180	1.180	1.40
.25	1.768	1.735	1.97
.30	2.603	2.571	2.80
.35	3.813	3.775	4.20
.40	5.596	5.436	6.18
.45	8.276	7.641	8.90
.50	12.399	10.477	12.50

Comparison of the results of the present work with results obtained by purely mathematical procedures in reference 8 is of considerable interest. Briefly, boundary collocation procedures were applied to a suitable stress function to obtain values of the stress intensity factor corresponding to various values of a/W for a single-edge-notch specimen under a given, uniformly distributed load. Values of $(E/2)[dC/d(a/W)]$ derived from these results are compared in table VI with corresponding values from the present work. Values from reference 7 are also listed.

In the range of values of a/W between 0.20 and 0.40, the stress-function solution results are in excellent agreement with the present experimental results. The discrepancies between values below this range are probably mainly attributable to inaccuracy of the experimental results. Only two measurements were made in this lower range; furthermore, the compliance is quite insensitive to a/W in this range. The discrepancies between values corresponding to a/W greater than 0.4 probably arise for a different reason, although, again, only two measurements were made in this higher range. The reason suggested is the bending of the calibration specimen that was referred to in the section Compliance Measurement Procedure. No account is taken of this bending in the stress function treatment that assumes that the shape of the specimen is unaltered by loading.

The bending decreases the eccentricity of loading with respect to the remaining cross section in the plane of the slot. The compliance for a given slot length is therefore slightly less than if the specimen were not allowed to bend. Since the effect is greater the greater the slot length, the values of $(E/2)[dC/d(a/W)]$ derived from the experimental data would be expected to be progressively smaller than those derived from the stress function treatment. Table VI shows this to be true. It should be appreciated that in this particular respect the experimental calibration values are probably more representative of a specimen in an actual test, which will suffer bending in the same manner as the calibration specimens.

The results of measurements of the extent of bending are shown in figure 5. When expressed, as here, in terms of the angle of bend per 1000 pounds load against a/W , there is no significant difference between results for specimens of different lengths (when the relatively insensitive method of measurement is considered). For a given bend angle, however, the effect on the

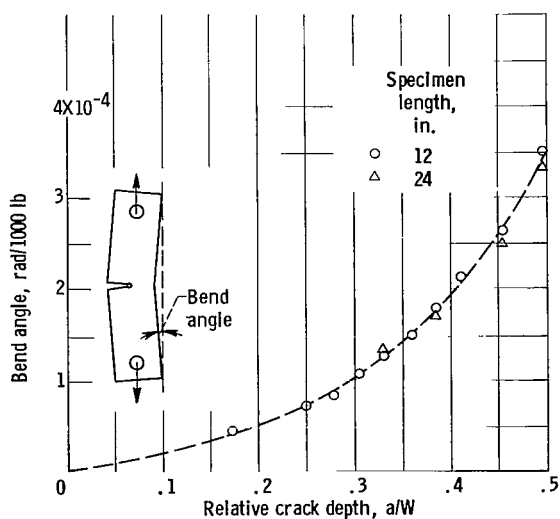


Figure 5. - Magnitude of specimen bending as function of relative crack depth.

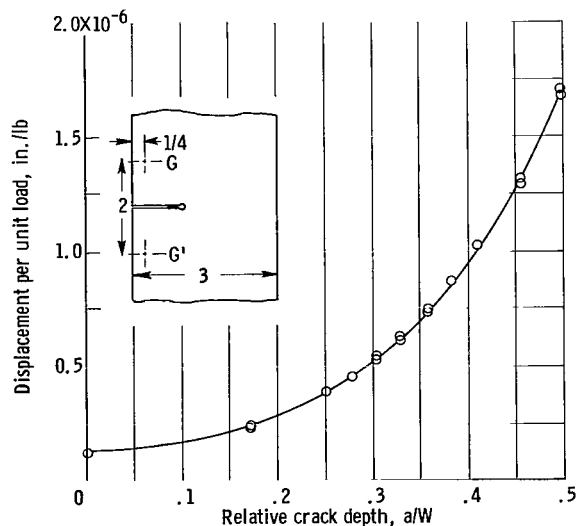


Figure 6. - Displacement per unit load between the gage points G and G' as function of relative crack depth for 3- by 12-inch aluminum 7075-T6 calibration specimens.

eccentricity of loading is proportional to the specimen length, or, more accurately, the distance between loading centers. Therefore it would be expected that the values of the rate of change of compliance with relative crack length would be somewhat smaller for a long specimen than for a short one. Comparison of tables IV and V will show that the values for the 24-inch specimen are, on an average, about 3 percent smaller than those for the 12-inch specimens. Furthermore, table VI shows that the values obtained with a specimen having a ratio of length to width of about 2 are consistently higher than the values obtained with the 12- by 3-inch specimens.

Crack Extension Detection Measurements

When K_{Ic} tests are conducted, some means of detecting onset of rapid crack extension in the opening mode must be used so that the load at which this occurs may be recorded. A load-displacement record similar to the ones used for calibration would serve this purpose since the record would be almost linear so long as no crack extension had occurred, but it would deviate increasingly from linearity with progressive crack extension. A step in the record would indicate temporary instability in the sense of appreciable crack extension with no change in load. Such an event has been referred to as pop-in of the crack (ref. 6). For this purpose the displacement change need not be measured between positions on the axis of the specimen; any pair of positions symmetrically disposed with respect to the crack will serve. In fact, it is convenient in testing single-edge-notch specimens to mount a displacement gage straddling the crack essentially at the edge of the specimen, as indicated in the inset sketch of figure 6. In the present work, a 2-inch-gage-length microformer extensometer was used as indicated to obtain load-extension records concurrently with the compliance calibration data. The results are plotted in figure 6, which is thus a calibration curve for a crack extension detection gage mounted in the position indicated.

CONCLUDING REMARKS

An accurate calibration was established for a single-edge-notch crack toughness specimen having a ratio of length to width of 4 by means of experimental compliance measurements. The calibration is given in table V in dimensionless terms that are applicable to a specimen of any material and thickness having the proportions of the smaller of the two specimens shown in figure 1, page 5. For crack toughness testing, a slot ending in a sharp crack would be used rather than the slot configuration shown in figure 1, but the effect of this difference on the calibration is negligible. The calibration accuracy in the range of greatest practical interest, relative crack length a/W where a is the crack length and W is the width of a single-edge-notch specimen, between 0.25 and 0.40, is estimated to be of the order of $\pm 1/2$ percent, which is ample for purposes of crack toughness testing.

The results of this experimental calibration have been compared with results obtained by the purely mathematical procedure of boundary collocation applied to a suitable stress function in a parallel investigation. Over the

range of values of a/W between 0.20 and 0.35, the agreement is within 1.3 percent, at a/W equal to 0.40, the agreement is within 3 percent (table VI). Greater discrepancies at larger values of a/W are attributed to the effect of specimen bending, which is not accounted for in the mathematical analysis.

It was established in preliminary experiments on a specimen of double length that the rate of change of compliance with relative crack length was virtually independent of the gage length over which the compliance measurements were made when the gage length was equal to or greater than twice the width of the specimen. The gage length used in the actual calibration measurements was $8W/3$.

Lewis Research Center

National Aeronautics and Space Administration

Cleveland, Ohio, May 18, 1964

REFERENCES

1. ASTM Special Committee: Fracture Testing of High-Strength Sheet Materials, pt. I. ASTM Bull. 243, Jan. 1960, pp. 29-40; pt. II, ASTM Bull. 244, Feb. 1960, pp. 18-28.
2. Irwin, G. R.: Fracture. Vol. VI - Elasticity and Plasticity. Encyclopedia of Phys., S. Flügge, ed., Springer-Verlag (Berlin), 1958, pp. 551-590.
3. Irwin, G. R.: Fracture Mechanics. Structural Mechanics, Proc. of First Symposium on Naval Structural Mechanics, J. Norman Goodier and Nicholas J. Hoff, eds., Stanford Univ., Aug. 11-14, 1958, Pergamon Press, 1960, pp. 557-594.
4. Irwin, G. R., and Kies, J. A.: Critical Energy Rate Analysis of Fracture Strength. Welding Jour. Res. Supplement, vol. 33, 1954, pp. 193s-198s.
5. ASTM Special Committee: The Slow Growth and Rapid Propagation of Cracks. Materials Res. and Standards, vol. 1, no. 5, May 1961, pp. 389-393.
6. Boyle, R. W., Sullivan, A. M., and Krafft, J. M.: Determination of Plane Strain Fracture Toughness with Sharply Notched Sheets. Paper 62-MET-13, ASME, 1962.
7. Sullivan, A. M.: New Specimen Design for Plane-Strain Fracture Toughness Tests. Materials Research and Standards, vol. 4, no. 1, Jan. 1964, pp. 20-24.
8. Gross, Bernard, Srawley, John E., and Brown, William F., Jr.: Stress Intensity Factors for a Single-Edge-Notch Tension Specimen by Boundary Collocation of a Stress Function. NASA TN D-2395, 1964.

9. Aiken, A. C.: Statistical Mathematics. Second Ed., Ch. IV, sec. 63 - Nonlinear Regression. Oliver and Boyd (London), 1942.

2/2/25
G

"The aeronautical and space activities of the United States shall be conducted so as to contribute . . . to the expansion of human knowledge of phenomena in the atmosphere and space. The Administration shall provide for the widest practicable and appropriate dissemination of information concerning its activities and the results thereof."

—NATIONAL AERONAUTICS AND SPACE ACT OF 1958

NASA SCIENTIFIC AND TECHNICAL PUBLICATIONS

TECHNICAL REPORTS: Scientific and technical information considered important, complete, and a lasting contribution to existing knowledge.

TECHNICAL NOTES: Information less broad in scope but nevertheless of importance as a contribution to existing knowledge.

TECHNICAL MEMORANDUMS: Information receiving limited distribution because of preliminary data, security classification, or other reasons.

CONTRACTOR REPORTS: Technical information generated in connection with a NASA contract or grant and released under NASA auspices.

TECHNICAL TRANSLATIONS: Information published in a foreign language considered to merit NASA distribution in English.

TECHNICAL REPRINTS: Information derived from NASA activities and initially published in the form of journal articles.

SPECIAL PUBLICATIONS: Information derived from or of value to NASA activities but not necessarily reporting the results of individual NASA-programmed scientific efforts. Publications include conference proceedings, monographs, data compilations, handbooks, sourcebooks, and special bibliographies.

Details on the availability of these publications may be obtained from:

SCIENTIFIC AND TECHNICAL INFORMATION DIVISION
NATIONAL AERONAUTICS AND SPACE ADMINISTRATION

Washington, D.C. 20546